Environmental Science & Technology

pubs.acs.org/est

Article

Unpiloted Aircraft System Instrument for the Rapid Collection of Whole Air Samples and Measurements for Environmental Monitoring and Air Quality Studies

Elizabeth Asher,* Alan J. Hills, Rebecca S. Hornbrook, Stephen Shertz, Stephen Gabbard, Britton B. Stephens, Detlev Helmig, and Eric C. Apel

Cite This: *Environ. Sci. Technol.* 2021, 55, 5657−5667

Read Online

ACCESS | Metrics & More | Article Recommendations | Supporting Information

ABSTRACT: A new airborne system, the Whole Air Sampling Pilotless Platform (WASPP), is described for the collection of whole air samples and in situ meteorological measurements onboard a commercial hexacopter. Rapid sample collection enables the collection ≤15 air samples per flight in positively pressurized miniature canisters, subsequently analyzed on a mated analytical system for up to 80 nonmethane volatile organic compounds (VOCs). The WASPP is well suited to investigate VOC gradients in urban environments impacted by traffic, industry, and oil and natural gas (O&NG) development, but has the sensitivity to characterize continental background conditions, as shown here using a subset of >40 species. We document empirical tests to minimize the influence of rotor wash and other sampling artifacts and report favorable results of laboratory-based calibrations of the WASPP's meteorological sensors and field-based comparisons of WASPP's VOC measurements and horizontal wind velocity measurements. Airborne WASPP measurements can complement and enhance ground-based VOC monitoring efforts by providing substantial meteorological and VOC measurement capability across vertical and horizontal spatial scales. These measurements reveal strong vertical gradients in VOC mixing ratios, depending on local meteorology and sources. WASPP has wide applicability for pollution source identification and quantification of hazardous air pollutants and precursors of criteria pollutants, including monitoring O&NG emissions or industry fenceline monitoring.

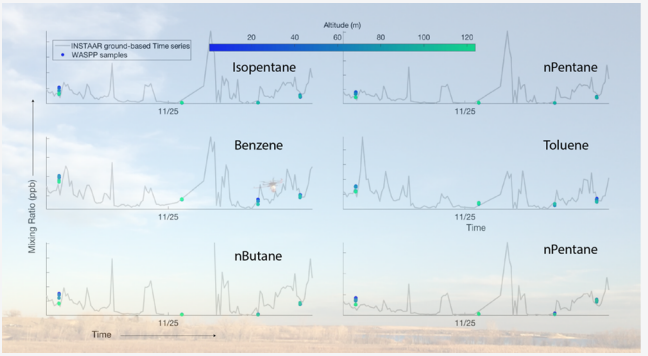

1. INTRODUCTION

In the United States, the Clean Air Act sets standards for concentrations of ground-level pollutants, such as ozone (O_3) and particulate matter (PM), which determine air quality and have been linked to respiratory, cardiovascular, and reproductive diseases.[1] Nonmethane volatile organic compounds (NMVOCs; typically and hereafter referred to as VOCs) play a primary role in the photochemical reactions that lead to the formation of both tropospheric O_3 and PM. Their distributions must be well understood to model regional air chemistry and predict air quality. VOCs also include regulated hazardous air pollutants (HAPs), such as acetaldehyde, acrolein, and benzene.[2] VOCs are emitted from a variety of sources, including motor vehicles, chemical manufacturing facilities, refineries, factories, consumer and commercial products, and natural (biogenic) sources (trees, grasses, shrubs). The types and classes of VOCs that provide the largest amount of reactivity vary by region. In the Southeastern U.S., biogenic species play a large and often dominant role, whereas areas in the Western U.S. may be highly impacted by emissions from oil and natural gas (O&NG) extraction and processing.[3]

Meteorological factors including wind velocity, atmospheric boundary layer (ABL) height, and turbulence, all of which are temporally and geographically variable, affect the exposure risk to harmful pollutants at ground level.[4] Ground-based VOC measurements cannot measure near-surface vertical gradients in VOCs or other pollutants and do not represent the composition of air aloft when the surface becomes decoupled from the residual nighttime boundary layer in the late afternoon or early evening. Characterizing background pollution, which may be entrained into the boundary layer where it mixes with local pollution, remains a major challenge for air quality forecasting.[5,6] Outflow from large metropolitan centers can alter the regional background mixing ratios of ozone and PM precursors, influencing VOC vertical gradients

Received: October 29, 2020
Revised: March 30, 2021
Accepted: March 31, 2021
Published: April 21, 2021

Downloaded via NOAA CENTRAL LIBRARY on August 17, 2022 at 15:40:23 (UTC).
See https://pubs.acs.org/sharingguidelines for options on how to legitimately share published articles.

ACS Publications

© 2021 The Authors. Published by American Chemical Society

hundreds of kilometer downwind.[7] Weather research forecasting models with chemistry and next-day air quality forecasts both improve considerably when airborne observations that resolve vertical gradients are included.[6,8]

Vertically resolved observations from crewed aircraft, balloons, and tall towers have been instrumental in constraining atmospheric models and in providing top-down VOC emission estimates but each has its limitations.[9−14] Numerous urban-air quality studies have employed tethered balloon sampling for VOCs, other trace gases, and meteorological parameters to better understand the evolution of tropospheric ozone over urban environments.[9,10,15,16] Data from the Boulder Atmospheric Observatory (BAO) tall tower, located in Colorado between 1977 and 2016, demonstrated that reported "bottom-up" VOC emission inventories underestimate contributions from O&NG extraction.[12] Compared to crewed aircraft, balloons and tall towers have limited ability to characterize the horizontal variance in vertical gradients. Helium balloons have become increasingly expensive to deploy due to a global shortage of helium, and hydrogen balloons present logistical challenges. The National Oceanic Atmospheric Administration Earth System Research Laboratory Global Monitoring Division (NOAA ESRL/GMD) tall tower network (defined as >50 m in height by NOAA) only includes six towers across the country, and only a handful of structures >400 m exist in the western United States.[6] Yet crewed aircraft are expensive to operate and opportunities to fly below 500−1000 feet are limited by Federal Aviation Administration (FAA) regulations.

Small, uncrewed aircraft systems (UAS) are increasingly capable of resolving the vertical and horizontal gradients in trace gases previously addressed by tethered balloons, tall towers, and crewed aircraft.[17,18] Yet payload weight and balance concerns remain paramount for UAS samplers: state-of-the art gas analyzers, such as proton-transfer-reaction mass spectrometers, gas chromatography mass spectrometers, and cavity ring-down-spectroscopy instruments greatly exceed the weight, size, and power limitations for small UAS. Existing UAS samplers for trace gases deployed from commercially available UAS include the actively pressurized version of the AirCore Sampling System,[19,20] an individual 2 L evacuated stainless steel canister for air sampling,[18,21] and several absorbent cartridge systems.[22] Similar sampling systems exist for the collection of three or more water samples from small UAS.[23] These systems have been deployed on relatively inexpensive ($1−5k) commercial multirotor UAS, which offer a unique and unprecedented combination of the abilities to execute exact maneuvers and to automatically maintain a stable hover, seek to maximize flight time and distance and facilitate widespread use by the scientific community. The capability to make rapid and multiple measurements of a wide variety of VOCs on UAS has not been demonstrated. The limitations of existing UAS sampling systems, described above are as follows: the AirCore Sampling System is only suited for long-lived greenhouse gases such as CH_4, CO_2, and CO;[20,24] a single 2 L canister system has the obvious limitation of a single sample per flight;[18,21] and VOC cartridges require long sampling times (i.e., ≥10 min), sensitivity to moisture, and the low recovery for nonpolar compounds.[17,22] One other whole air sampler used for the analysis of methane isotopes only (not VOCs) has also been recently described, which also requires a custom-built UAS platform due to weight and balance concerns.[25] Several additional concerns with respect to sampling from a multirotor UAS have recently been outlined, including the influence of rotor wash, thermal heating, off-gassing of UAS materials, and insufficient airflow for sensors.[17,26]

In this paper, we describe a new system, the Whole Air Sampling Pilotless Platform (WASPP), and its first measurements in the Colorado Front Range. The WASPP collects up to 15 samples per ∼20 min flight for subsequent measurements of vertical gradients of VOCs, as well as in situ meteorological measurements of temperature (T), relative humidity (RH), pressure (P), and horizontal wind velocity. Each discreet whole air sample can be collected in approximately 8 s during the flight. When coupled to a mated analytical system, the system is capable of quantifying >50 VOCs per sample. Sensor and inlet placement onboard a commercial multirotor UAS were carefully considered and empirically evaluated to minimize sampling artifacts. Our measurements resolve structure in VOC gradients in the Colorado Front Range from the surface to 122 m (the FAA altitude limit for small UAS). We discuss the influence of vertical mixing and stratification, as well as horizontal transport in altering vertical distributions of VOCs. WASPP measurements show promise for source apportionment in an urban area impacted by ongoing oil and natural gas extraction and processing. Documenting the vertical structure of pollutants and precursors is an integral part of understanding regional air quality and the chemical evolution leading to ozone and PM formation downwind. We demonstrate that the WASPP system, coupled with its analytical analysis system, can provide some of the key high-quality meteorological and chemical measurements required to enhance our understanding of these processes.

2. METHODS

2.1. Description of the WASPP System and the Sample Extraction System. The WASPP instrument payload weighs 6.0 kg and includes an array of 8−15 100 mL canisters that can be pressurized inflight to 68.9 hPa above ambient pressure (yielding 180 mL of samples at STP), meteorological sensors, and an onboard computer (Figure 1). The instrument is mounted to a DJI Matrice 600 Pro (M600 Pro) frame using a Ronin MX gimbal (Figure 1a) to dampen shock to the electronics and other components. The M600 Pro platform can carry payloads up to 15 kg and has an excellent positioning system accurate to ±0.5 m in the vertical direction and ±1.5 m in horizontal directions, and good stability in moderate winds (≤8 m s^{-1}). The largest capacity M600 Pro batteries available (TB48S) enable a total flight time of ∼20 min for a 6.0 kg payload.

The WASPP measurements and sample collection are controlled and recorded at a resolution of ∼1 Hz using an RPi-2 model B and a custom electronic board (Figure 1a). The system has an ambient T and RH sensor (Vaisala HMP110) and an ambient P sensor (TE Connectivity EPRB-2; Figure 1a). T and RH are measured with total uncertainties (±1σ) of less than ±0.02 °C, ±1.1% (0−90% RH) and ±1.8% (90−100% RH), respectively. Ambient P is measured with a total uncertainty of ±0.018%. The WASPP also has a lightweight sonic anemometer, which we use to measure horizontal wind velocity (TriSonica Mini-WS, Sonic Anemometer; Figure 1b). Additional instrument electronics include a sample flow meter (Honeywell AWM5101VN), a sample pressure sensor (TE Connectivity EPRB-2), a GPS, and an analog input dedicated to monitoring system battery power (Figures 1a and S1).

https://doi.org/10.1021/acs.est.0c07213
Environ. Sci. Technol. 2021, 55, 5657−5667

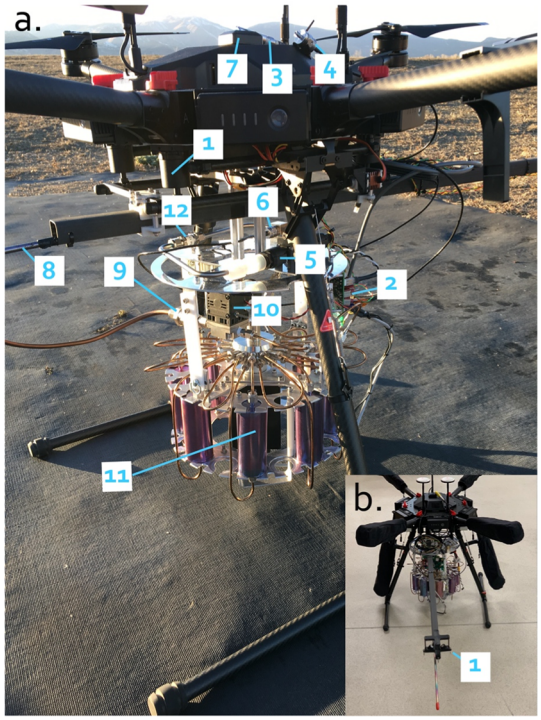

Figure 1. (a) Photo of the WASPP system, including various components: (1) the Ronin MX gimbal, (2) light-emitting diode (LED) outputs on a custom-made circuit board and onboard computer, (3) an ambient T and RH sensor, (4) an ambient pressure sensor, (5) flow meter, (6) system pressure sensor, (7) GPS antenna, (8) the inlet, (9) a 2 μm filter, (10) a KNF micro diaphragm gas pump, (11) the canister array, and (12) a check valve. See text for specific part numbers. (b) Photo of the (1) WASPP system's sonic anemometer on a boom near the air intake.

The internal plumbing of the WASPP miniaturized whole air sampling system as shown in Figure S1a is comprised of the inlet, a 2 μm stainless steel filter to remove particulates (Swagelok SS-4FW-2), a micro diaphragm gas pump (KNF NMP 850), a removable canister array of dual-ended canisters (Entech Inc., Silonite R), and a 68.9 hPa check valve on the system exhaust line (SS-4C-EP-15; Figures 1a and S1). Canisters can be flushed (nominally for >80 s) between waypoints and filled within 8 s at a flow rate of ∼1 slpm (SLM), measured downstream of the check valve.

Postflight the WASPP canister array is mated to an extraction system (Figures S1 and S2). This system consists of an RPi-2 computer and custom electronic board, a Swagelok pneumatic valve (SS-4BK-1C), a microelectric two-position valve (VICI ETMA 48727), a 24-VDC solenoid valve (Humphrey PN 31E1), and a mass flow controller (Tylan FC-280SAV) calibrated for 100 sccm N_2. These components allow the sequential transfer of the collected miniature canister samples to the National Center for Atmospheric Research (NCAR) Trace Organic Gas Analyzer (TOGA) at a flow rate of 60 sccm (Figures S1 and S2). Ultra-high-purity (UHP) N_2 (80 sccm) is used to flush the extraction system between canisters on the canister array to prevent any possible contamination between samples or with room air. TOGA is a custom-built fast gas chromatography mass spectrometer (GC/MS), capable of measuring >80 VOCs and achieves extremely low limits of detection (low pptv to high ppqv) with small sample sizes (<15 mL).[27] The extraction system's sample flow (60 sccm) is connected to the inlet bypass line from which TOGA subsamples this flow at a rate of 25 mL min^{-1} for ∼35 s into its cryogenic preconcentration system. Prior to the start of the TOGA analysis cycle, the 60 sccm sample flow preconditions the extraction system and TOGA inlet bypass for ∼20 s, requiring a total of ∼55 mL of sample for each VOC measurement. Extraction and analysis of each sample on TOGA (including sample purging and system flushing between samples) is completed within 2 min, allowing eight miniature WASPP canisters to be analyzed within 20 min. Positively pressurized miniature canisters contain enough gas to allow for two analytical measurements from each canister collected air sample.

2.2. Sensor and Inlet Placement. Multiple rotors induce complex turbulent airflows near UAS platforms, and rotor-wash eddies can impede representative measurements of the atmospheric parameters.[28] Depending on the measurement, potential multirotor UAS sampling artifacts may also include sensor thermal heating, insufficient sensor airflow, and off-gassing from UAS materials.[17,26] We used an experimental approach to identify sensor placement sites that minimize the influence of rotor wash and ensure sufficient airflow, conducting tests with a small, commercial T, RH, and P sensor (iMET-XQ2) mounted at various positions on the M600 Pro (Figure S2). Ambient measurements of T, RH, and P within the bottom 100 m of a well-mixed (i.e., turbulent) ABL should follow the −5/3 power law due to cascading kinetic energy from larger to smaller eddies.[29] We presume that deviations from the −5/3 power law reflect non-natural sources of turbulence and in this case the influence of rotor wash from the DJI M600 Pro, which could confound airborne measurements and yield less precise vertical gradients.[28] These tests took place in June between 10 AM and 3 PM local time in presumably well-mixed summertime ABLs (<122 m), over rural, flat grass pastures near a reservoir north of Boulder, Colorado (Figure S3).

We calculated the power spectra of 1 Hz T, RH, and P data for our three flight patterns (i.e., ascending profiles, descending profiles, or sustained hovers) and sensor position (Figure 2). Sensor positions included (1) centered, directly on top of the hexacopter, (2) at the multicopter's edge, above a M600 Pro battery and ≥15 cm horizontal distance from the rotors, and (3) on a boom ≥40 cm in front of and 5 cm below the rotors, oriented into the direction of the wind. Data obtained on ascending profiles from position 1 and on all flight patterns in position 3 have fewer frequency peaks either above or below the −5/3 power line, indicating that these combinations of sensor placements and flight patterns minimized non-natural sources of turbulence. We opted to locate the inlet and anemometer in position 3, on the boom, so that measurements and sample collection could take place during sustained hovers. This inlet position has the added benefit that VOC measurements here are less susceptible to potential off-gassing artifacts from plastics of the DJI M600 Pro.[17] On our science flights in November and December, sensors for ambient T, RH, and P were located in position 1 due to weight and balance concerns. To prevent the self-heating of sensors[26] and negate nonenvironmental heat sources, the HMP110 T and RH sensors were located >5 cm from the airframe (and nearby devices). Only data from ascending profiles were used to determine background meteorological conditions with ascent rates of >3 m s^{-1} to ensure sufficient airflow. Descending profile measurements in this position (and position 2) sample

https://doi.org/10.1021/acs.est.0c07213
Environ. Sci. Technol. 2021, 55, 5657−5667

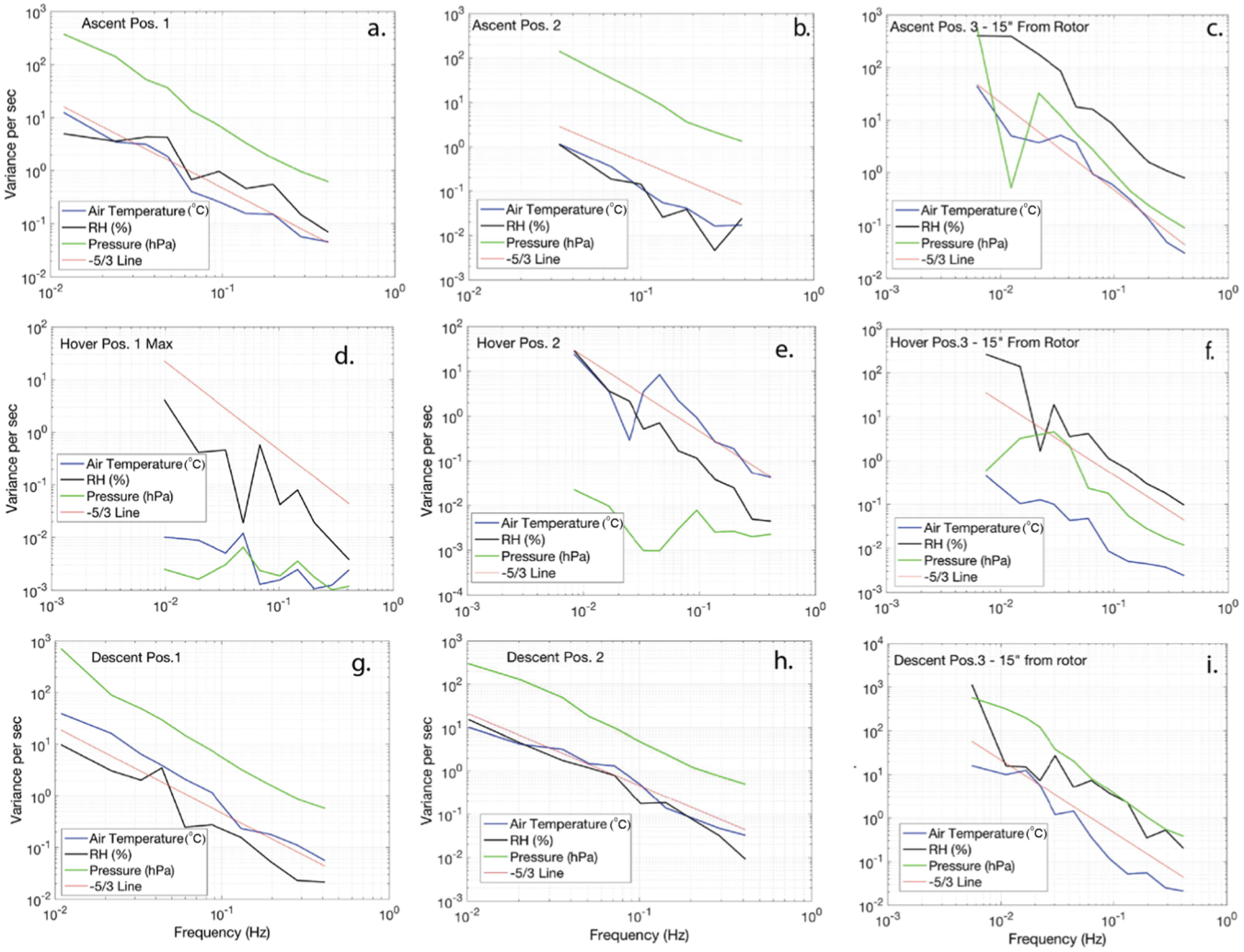

Figure 2. Comparisons of measured *T*, RH, and *P* during (a–c) ascents, (d–f) sustained hovers, and (g–i) descents. The locations of positions 1–3 are outlined in the text. Smoothing was done using a log increasing averaging technique in the frequency domain. In each panel, the reference −5/3 line (orange) shows the expected behavior for turbulent energy transfer in the inertial subrange of the energy spectrum.

rotor wash, although the airframe thrust and air speeds reach their inflight minimum in descent. The HMP110 *T* sensor is in large part shielded from direct solar radiation by a plastic grid filter, which with sizable slats permits good airflow and a fast response time. The EPRB-2 pressure sensor onboard the WASPP has a compensated temperature range from 0 to 100 °C, and all flights took place within this range.

Recent studies have documented a temperature bias ≥1 °C due to thermistor heating from the direct exposure to incoming solar radiation, particularly in calm conditions with high-incoming solar radiation.[30] Although we cannot rule out some potential bias in WASPP *T*, and subsequently RH (Figure S4c–e), we estimate that this bias would be ≤0.5 °C given the environmental conditions observed during our flights (typical wind speeds >3 m s^{-1} and lower solar radiation due to a combination of the sampling time of year, partial cloud cover and typical morning and late afternoon sampling times[26,30]). Our platform would benefit from an inflight *T* and RH intercomparison and future measurements, particularly those under different environmental conditions, from a now standard solar radiation shield.[26]

2.3. WASPP Sensor Calibrations and WASPP System Blanks. We calibrated WASPP's T, RH and *P* sensors in the NCAR Earth Observing Laboratory (NCAR/EOL) Calibration Laboratory. The WASPP HMP110 was thermostated in a temperature oil bath with six set points, ranging from −5 to 45 °C (accurate to within ±0.5 °C and stable to within ±0.0003 °C) (Figure S4a). The WASPP EPRB-2 pressure sensor was calibrated in line with the NCAR/EOL Calibration Laboratory's Ruska 7250i pressure controller and quartz bourdon tube reference pressure sensor (precision of ±1.7 mbar and a long-term stability, and accuracy ±1σ, of 1 ± 0.4 mbar) (Figure S4b). The HMP110 sensor was also enclosed in the Calibrations Laboratory's Thunder Scientific model 2500 humidity generator at three temperatures ranging from 0 to 45 °C, each with nine RH set points between 10 and 95% RH (accurate ±1σ of ±0.5%) (Figure S4c–e). Sensors showed excellent agreement compared to the references, although the accuracy of the HMP110 RH sensor decreased slightly at lower temperatures. We think these sensors should be calibrated semiannually for optimal performance.

WASPP miniature canister array blanks were conducted to establish the approximate detection limits (DLs) of the WASPP system with respect to 42 species. Extraction system blanks were tested routinely after field measurements. To determine canister array blanks, all eight miniature canisters in

https://doi.org/10.1021/acs.est.0c07213
Environ. Sci. Technol. 2021, 55, 5657–5667

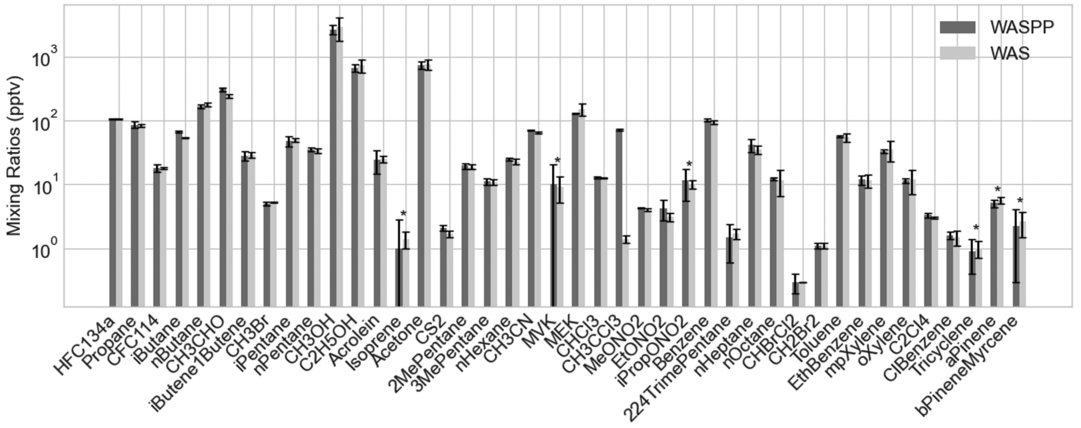

Figure 3. Comparison of three WASPP and three WAS ground-based samples. Error bars show the standard deviation (SD) of canister mixing ratios (of each type). Note the log scale to facilitate comparisons across several orders of magnitude.

the array were filled with UHP N_2 on February 5, 2021 and stored for between 0.5 and 1 h prior to analysis, which is similar to the transport and storage time of WASPP canister samples collected in the field to date, due to transit times of less than 20 min between sites and the NCAR Foothills Laboratory. The WASPP system uncertainties were assigned according to whichever was higher, the TOGA analytical DL, or the median WASPP canister blanks, all listed in Table S1. The WASPP DL were ≤5 ppt for light alkanes and aromatics, <0.5 ppt for biogenic VOCs, and <60 ppt for oxygenated VOCs, such as acetone, CH_3CHO, and methanol. Halogenated VOCs had low canister blanks and DL (<1 ppt) with the exception of CH_3CCL_3.

2.4. WASPP Field-Based Side-by-Side Comparisons. We conducted a side-by-side comparison between conventional 2 L whole air sampler (WAS) stainless steel canisters and the grounded WASPP for quality assurance of VOC measurements. Samples were collected in a three conventional 2 L canisters[31−33] and three miniature WASPP canisters on February 5, 2021 ∼30 m outside the NCAR Foothills Laboratory. The 2 L canisters and WASPP canisters were filled at 4:13, 4:15, and 4:17 PM. Both full-sized WAS and miniaturized WASPP canister samples were analyzed using TOGA. WASPP miniature canisters were analyzed within ∼1 h of collection, and the 2 L WAS canisters were analyzed within ∼2 h. Triplicate measurements were made from the 2 L canisters and duplicate measurements were made from the WASPP miniature canisters. We observed very good agreement between 40 species, including selected oxygenated VOCs, alkyl nitrates, halogenated VOCs, biogenic VOCs, and nonmethane hydrocarbons, on average biased high by 3.3%, with the exception of methyl chloroform (CH_3CCl_3; Figure 3). Given the large background in CH_3CCl_3 in N_2 blanks, we hypothesize that this compound is emitted from a component in the sampling system, and future work will seek to investigate the source of this CH_3CCl_3 contamination. In principle, the WASP, when mated to TOGA, can measure a substantial subset of the 80+ species that the in situ TOGA instrument can measure.[34,35] We conservatively put this figure at 50 species.

The performance of the WASPP miniature sonic anemometer inflight was evaluated by comparing it with a stationary R.M. Young sonic anemometer at a fixed height of 10 m over flat terrain on several days under different meteorological conditions. The wind velocity from each anemometer was corrected for the anemometer's compass heading, converted to U and V wind vectors, and arithmetically averaged over the 90 s sampling period. Horizontal wind velocity measurements differed by 0.20 ± 0.15 m s^{-1} and 12 ± 8° (mean ± SD) between the stationary anemometer and the WASPP Trisonica Mini anemometer (Table S3). Based on previous direct measurements of two-dimensional (2D) wind velocity using UAS borne sonic anemometers, we expect small biases in wind speed and wind direction, particularly during quiescent periods,[36,37] despite our sampling from minimally perturbed airspace (shown here using our experimental approach; Section 2.2 and elsewhere using computational fluid dynamics (CFD) simulations for the DJI and similar multirotor UAS[22,25]). Though fixed-wing multihole probe and fixed tower anemometer measurements remain the best means of providing three-dimensional (3D) winds for air quality forecasting,[38] the anemometer measurements described here prove useful for the interpretation of air quality and environmental monitoring VOC measurements.

2.5. Description of Sampling Sites. Airborne measurements from 11 vertical profiles took place in November and December 2018 at two locations: 0.2 miles northwest of the Boulder Reservoir, and in Broomfield County, 14 miles southeast of the Boulder Reservoir (Figure S3). Flights in Broomfield County took place over a recently harvested wheat field, adjacent to other fields and two major highways, at the southern end of a region with oil and gas wells (Figure S3).[39] Elevated mixing ratios of anthropogenic VOCs are frequently observed near the surface at the Boulder Reservoir due to its proximity to the city of Boulder and to agricultural and O&NG activities in the Colorado Front Range.[39]

2.6. Pairing Airborne WASPP and Nearby Ground-Based Time-Series Measurements. We used nearby VOC and meteorological time-series records to show how WASPP airborne measurements could be a good addition to ground-based research campaigns. Ground-based VOC measurements were made by the Institute of Arctic and Alpine Research (INSTAAR) in collaboration with the Colorado Department of Public Health and Environment (CDPHE) and sponsored by Boulder County Public Health at the Boulder Reservoir in November and December 2018.[39] The INSTAAR site is located across the Boulder Reservoir approximately 1.3 miles from the WASPP measurement site (Figure S3). The ground-based measurements are made using a preconcentration system and an automated gas chromatograph with a flame-ionization

https://doi.org/10.1021/acs.est.0c07213
Environ. Sci. Technol. 2021, 55, 5657−5667

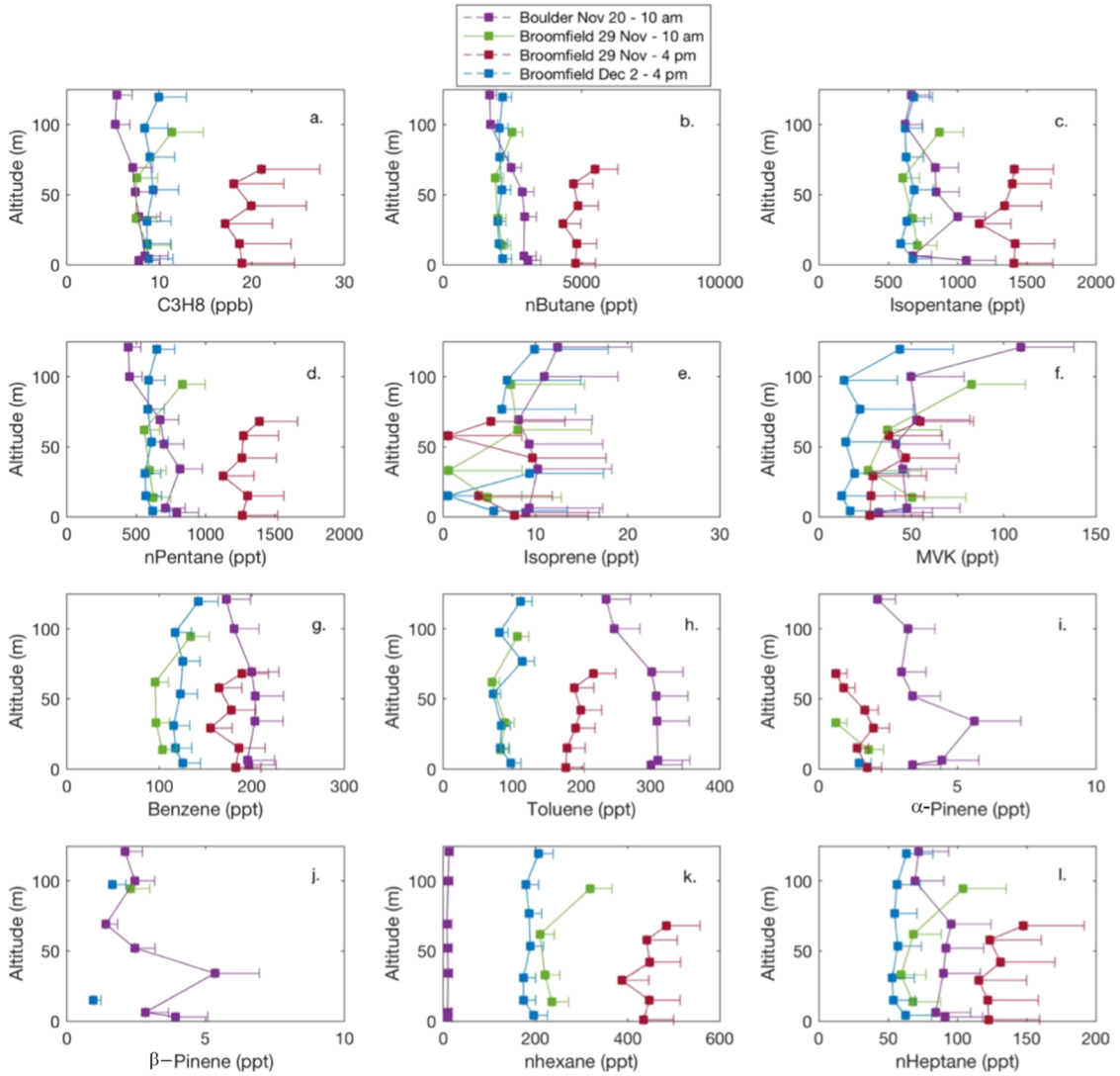

Figure 4. Detailed profiles of VOCs with altitude from the WASPP system on November 20 at 11:10 am, November 29 at 10:15 am, November 29 at 4:10 pm, and December 2 at 4:00 pm. Error bars represent whichever is greater, the standard deviation of duplicate measurements (subsamples from a single miniature canister), or the total WASPP uncertainty (symmetric error is only shown in a positive direction for clarity; Table S1). Note differences in scale (ppt vs ppbv) on the *x*-axes.

detector,[40] which requires 10 min for sample collection. Air was aspirated through a 6.4 mm stainless steel inlet at a fixed height of 5 m and a flow rate of 1.5 L min^{-1} for VOC analysis. The instrument was calibrated approximately every 4 days in 2018, and blank subtraction for benzene and toluene were determined based on system measurements of zero scrubbed air. The calibrations are referenced against the World Meteorological Organization (WMO) Global Atmospheric Watch (GAW) scales for VOCs. Hourly temperature and wind velocity data were also obtained courtesy of CustomWeather, which compiles weather records from airports, WMO, and MADIS weather stations (https://www.timeanddate.com/weather/forecast-accuracy-time.html).

3. RESULTS AND DISCUSSION

3.1. VOC Mixing Ratios. The WASPP system reveals temporal variability and vertical gradients in nonmethane hydrocarbons within the ABL (Figure 4) that highlight the utility of frequent vertical profile VOC sampling. Vertical gradients on the afternoons of November 20, November 29, and December 2, 2018 show surface enrichments of light alkanes and aromatics, and in some cases biogenic compounds (e.g., November 20). Our data suggest that large accumulations of VOCs may develop rapidly, as shown in the difference between measurements of anthropogenic VOCs from samples collected on the morning and afternoon of November 29. Similar vertical gradients in anthropogenic C_3−C_6 alkanes and aromatics suggest common local or regional sources (e.g., December 2; Figure 4a−d,g−h,k). WASPP samples also provide evidence of routinely elevated mixing ratios of C_3−C_6 alkanes as high as 120 m (Figure 4). Light alkanes and benzene have relatively long lifetimes (3 days to 2 weeks with [OH] of 5×10^{-5} cm^{-3}), compared to many biogenic VOCs with photochemical lifetimes of a few hours, such as isoprene and monoterpenes.

Throughout this study, mixing ratios of C_3−C_6 alkanes were well correlated with one another (r^2 = 0.81−0.96; $p < 0.001$), weakly correlated with aromatics (r^2 = 0.36−0.44; $p < 0.001$), and negatively correlated or uncorrelated with biogenic compounds (Table S2). Mixing ratios of light alkanes and

https://doi.org/10.1021/acs.est.0c07213
Environ. Sci. Technol. 2021, 55, 5657−5667

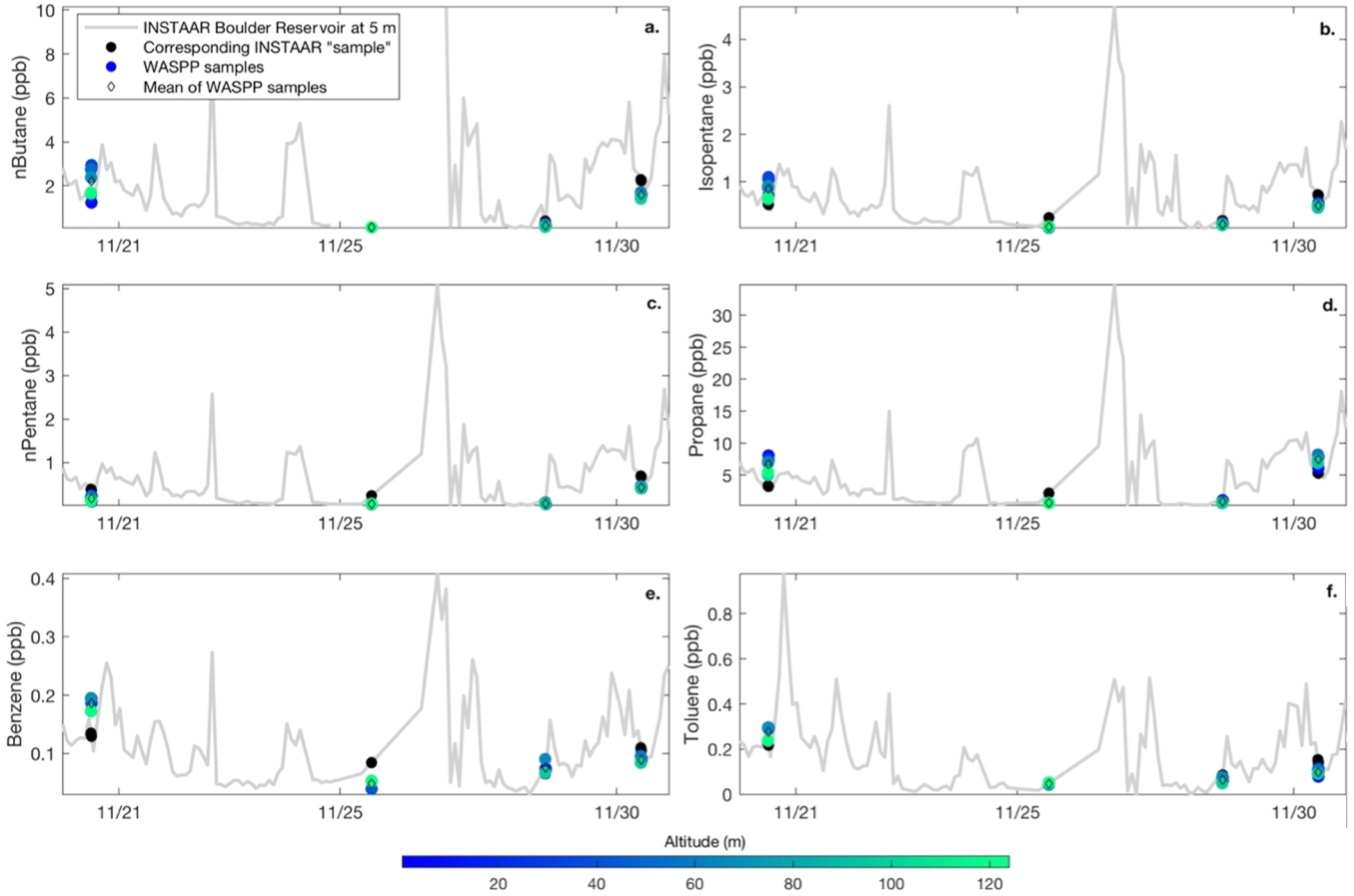

Figure 5. Comparison of the WASPP vertical profiles at the Boulder Reservoir, and the mean mixing ratios of all samples in the vertical profiles, to measurements at the nearby Boulder County/INSTAAR site. Hourly Boulder County/INSTAAR measurements (samples are collected over a 10 min period) were made from a height of 5 m. WASPP measurements and those at the INSTAAR site were significantly correlated for all compounds with relatively low mean absolute error (MAE): *n*-butane (r^2 = 0.37; p < 0.01; MAE = 0.096 ppb), isopentane (r^2 = 0.38; p < 0.01; MAE = 0.02 ppb), *n*-pentane (r^2 = 0.91; p < 0.001; MAE = 0.20 ppb), propane (r^2 = 0.73; p < 0.001; MAE = −1.7 ppb), benzene (r^2 =0.69; p < 0.001; MAE = -7.9×10^{-3} ppb), and toluene (r^2 =0.83; p < 0.001; MAE = 3.8×10^{-3} ppb) (see Figure S3 for geographical location of sites).

aromatics ranged from less than one to tens of parts per billion and tens to hundreds of parts per trillion, respectively (Table S2). Biogenic nonmethane hydrocarbons were also weakly correlated with one another (r^2 = 0.23−0.69; p < 0.001; Table S2), likely due to both disparate natural sources and short atmospheric lifetimes. Mixing ratios of biogenic alkenes ranged from less than one part per trillion to tens of parts per trillion (Table S2). These concentrations are generally in line with those from previous airborne observations[12,13,41] and demonstrate the wide analytical range (<10−25 ppb) of the WASPP system when used in conjunction with TOGA.

3.2. Role of Vertical Mixing and Horizontal Transport in Observed VOC Distributions. In addition to local sources and background mixing ratios, ABL mixing and stratification as well as horizontal transport may rapidly alter distributions of chemical species. The WASPP flights in November and December 2018 took place under a range of stable, quiescent to actively mixing and/or windy meteorological conditions (T ranged from 3 to 22 °C and RH ranged from 14 to 64%; Figures S5 and S6). Horizontal wind speeds generally increased with altitude, as expected (Figure S6b−d),[42] reconfirming how air masses at altitude are often transported greater distances and thereby reflect larger regional footprints. Below, we discuss two examples of how the WASPP's in situ meteorological measurements can help interpret the observed vertical VOC distributions and show that the WASPP will be a useful addition to ground-based campaigns.

A well-mixed ABL and warm, but breezy conditions may not necessarily prevent the development of vertical gradients in VOCs. For example, on November 20 and 25, the decreasing θ with altitude and higher RH near the surface indicate active mixing in the ABL and evapotranspiration (Figure S5a−d). Yet at 10 am on November 20, we observed vertical variability and boundary layer enrichments in α-pinene, β-pinene, isoprene, benzene, toluene, and other compounds (Figure 4g−j). Wind shear, indicated by a shift in wind direction from W to E on November 20 at 50 m altitude at the Boulder Reservoir (Figure S6b) may have contributed to the observed near-surface enrichments of monoterpenes. The Boulder Reservoir site is located due east of evergreen forests on the Colorado Foothills. Conversely, active mixing and strong easterly winds on November 25, with no wind shear observed on this day, led to nearly uniform mixing ratios in VOCs (Figure S6c). Wind shear (e.g., Figure S6b,d) has the potential to strongly influence vertical distributions of VOCs by transporting air masses from different source regions to a site.

Cold, quiescent conditions impede vertical mixing, as well as horizontal advection, and the dispersion of local emissions. As noted in Section 3.2, well-mixed vertical VOC distributions on the morning of November 29 gave way later in the day to

https://doi.org/10.1021/acs.est.0c07213
Environ. Sci. Technol. 2021, 55, 5657−5667

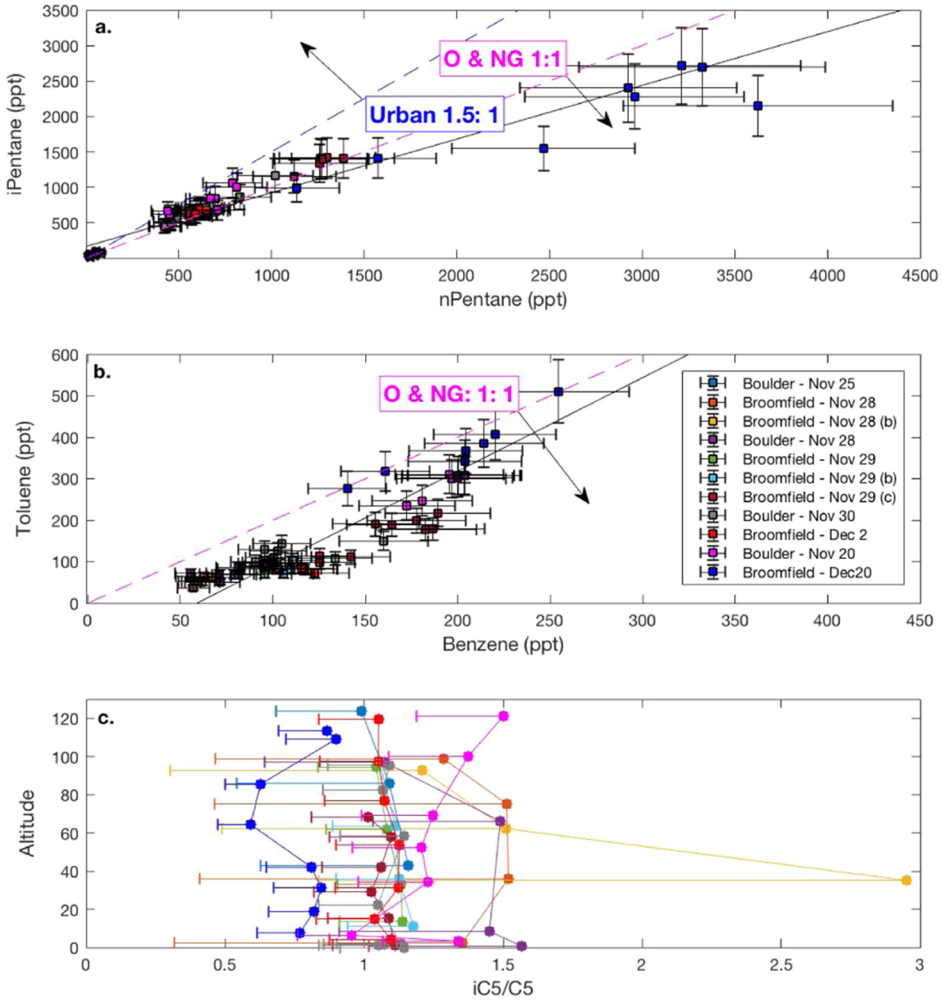

Figure 6. Isopentane/*n*-pentane (iC5/C5 with lines denoting the boundaries of urban (1.5:1) vs O&NG (1:1) influences (a), toluene/benzene), toluene/benzene (tol/benz) with a line denoting the typical boundary of O&NG influences (2:1) (b) of WASPP airborne observations. Line of best fit for iC5/C5 and tol/benz, based on ordinary least square (OLS) regressions, is also shown (iC5 = (0.72 ± 0.04) C5 +210 ± 48; r^2 = 0.93; p = 5.3 × 10^{-22}; tol = (2.0 ± 0.17) benz −110 ± 25; r^2 = 0.79; p = 1.2 × 10^{-13}). Vertical profiles of the iC5/C5 ratios with altitude from all flights (at both locations) are shown in (c). As in Figure 4, the error bars represent whichever is greater, the standard deviation of duplicate measurements (subsamples from a single miniature canister), or the total WASPP uncertainty—in (c); the symmetric error is only shown in the negative direction for clarity.

overall higher mixing ratios and near-surface (<20 m) enrichments in light alkanes, such as isopentane, *n*-pentane, *n*-hexane, *n*-heptane, and propane, as well as benzene (Figure 4a,c,d,i−k). The afternoon vertical profiles of RH and θ, which increased slightly with altitude, suggested that any active mixing earlier that day had ceased by that afternoon to form a stable ABL and facilitate rapid surface enrichment in VOCs (Figures S5f,h and 4). Decreasing northwesterly winds throughout November 29 also allowed for the rapid near-surface accumulation in anthropogenic VOCs (Figures 4 and S6d,e).

The airborne WASPP observations can complement existing ground-based field campaigns. INSTAAR ground-based measurements southeast of the Boulder Reservoir track the temporal variability in near-surface mixing ratios of several nonmethane hydrocarbons, namely, propane, *n*-butane, isopentane, *n*-pentane, benzene, and toluene. WASPP airborne observations of these VOCs provide additional insight with snapshots of the vertical variability and the mean state of the lower 120 m of the ABL (Figure 5). Overall, mixing ratios of WASPP samples from vertical profiles northwest of the Boulder Reservoir and the nearby ground-based INSTAAR measurements appeared consistent with one another, and ordinary least square (OLS) regressions between samples from each platform support this agreement (Figure 5). To some extent, differences between WASPP measurements and those from the INSTAAR site may reflect horizontal gradients as well as vertical variability in anthropogenic VOC mixing ratios. We note that similar times for sample collection between the INSTAAR system and the WASPP facilitate this comparison; ground-based WAS collected with intervals of days to weeks might not benefit as much from the addition of airborne WASPP observations.

3.3. Potential for Source Apportionment Using WASPP Samples. Quantifying enrichment ratios is particularly advantageous when it is not possible to directly quantify VOC emissions from every source. A comprehensive overview indicates that VOC sources in the Colorado Front Range are dominated by mobile emissions and other industries within Denver and by O&NG in the counties to its north.[41] Ratios of isopentane/*n*-pentane (iC5/C5) from whole air canister samples have been used to distinguish between O&NG and

https://doi.org/10.1021/acs.est.0c07213
Environ. Sci. Technol. 2021, 55, 5657−5667

urban emissions. An iC5/C5 of 0.8−1.0 is consistent with O&NG emission,[41,43,44] whereas a higher ratio of 1.5−2.5 indicates urban emissions (ratios between these two ranges imply a mix of sources) and a lower ratio (0.3−0.5) is associated with fire emissions. The iC5/C5 from fresh vehicle exhaust emissions may be as high as 3.8−4.5.[44,45] Automobile emissions also typically have high ratios of toluene/benzene (≥2), compared to O&NG emissions.[41,43,46]

Similar to crewed aircraft observations and tall tower measurements, which have larger regional footprints than ground-based measurements, the WASPP VOC observations may be used to characterize regional source signatures. We observed largely consistent ratios of iC5/C5 across our flights that fall within the range of observations from previous studies (Figure 6a).[41,43,44] We observed less scatter in iC5/C5 than for tol/benz using OLS, likely due to differences in chemical lifetimes (Figure 6a,b). Whereas benzene has a chemical lifetime more than 4 times that of toluene, isopentane and *n*-pentane both have nearly identical chemical lifetimes of approximately 5 days. As a result, the age of the air mass will disproportionately impact tol/benz, compared with iC5/C5. Our data indicate that airborne WASPP samples were influenced by a mix of O&NG emissions and urban-air masses (Figure 6a,c). We observed consistent iC5/C5 between 1 and 1.5 on most of our flights, although a few samples appeared impacted primarily by urban emissions (iC5/C5 > 1.5; e.g., on flights on November 28 in Boulder and Broomfield) and one flight appeared to be primarily influenced by O&NG emissions (iC5/C5 < 1; e.g., on December 20 in Broomfield County). Given that the Weld County O&NG region extends east/northeast of Boulder and Broomfield County, our November 28 results are consistent with transport of air masses not impacted by the O&NG region via westerly winds, whereas northeasterly winds transported air from the O&NG region on 20 December to the WASPP sampling location (Figures 6 and S6c,e). Rigorous source attribution would require more flights and detailed analysis.

4. CONCLUSIONS

The WASPP is a unique low-cost, highly capable UAS platform that measures ambient *T*, RH, *P*, and 2D winds and can rapidly collect up to 15 whole air samples for subsequent analysis of up to 50 VOCs per sample. We demonstrate that the airborne WASPP measurements complement and enhance near-surface VOC monitoring efforts by providing substantial meteorological and VOC measurement capability across vertical (typically up to 122 m) and horizontal spatial scales and show that the system should have wide applicability for pollution source identification. We envision that this technique will be an important complement to systems measuring air pollutants at the fenceline or in communities near industrial facilities and can help identify and provide feedback for mitigation of air pollution that may drift across property lines. Moving forward, the WASPP could also aid in validating large-eddy simulations and air quality forecasting models[6,47] and enable the calculation of mass balance flux estimates near large VOC sources. Population in the Colorado Front Range is rapidly growing, and the region is being impacted by climate change and sustained O&NG extraction and processing activities. These regional shifts result in concomitant changes and redistributions of emission sources which, in turn, cause changes in the amount and distributions of the photochemical products, ozone, and PM of these emissions. The WASPP system and complementary UAS systems can play an important role in airborne measurements to accurately assess the import and export of emissions, locally and regionally, that are either HAPs or directly impact criteria pollutants. UAS will become an increasingly useful tool for scientific monitoring as battery technology improves and the FAA grows more accustomed to regulating UAS traffic.

■ ASSOCIATED CONTENT

Supporting Information

The Supporting Information is available free of charge at https://pubs.acs.org/doi/10.1021/acs.est.0c07213.

TOGA detection limits, WASPP mini-can blanks, and WASPP system uncertainties (Table S1); VOC mixing ratios (mean and range) and statistically significant correlation coefficients of VOC measurements on all WASPP flights (Table S2); WASPP Trisonica Mini anemometer and Young sonic anemometer side-by-side comparison (Table S3), a detailed schematic of WASPP system plumbing and extraction system plumbing (Figure S1); labeled photo of extraction system components (Figure S2), map of WASPP sampling sites and other existing and previous VOC sampling sites (Figure S3); laboratory sensor calibration of the WASPP's *P*, *T*, and RH sensors (Figure S4); WASPP vertical profiles of RH and θ from four different flights (Figure S5); and WASPP vertical profiles of wind vectors from four different flights (Figure S6) (PDF)

■ AUTHOR INFORMATION

Corresponding Author

Elizabeth Asher − *Atmospheric Chemistry Observations & Modeling Laboratory, National Center for Atmospheric Research, Boulder, Colorado 80301, United States; Earth Observing Laboratory, National Center for Atmospheric Research, Boulder, Colorado 80301, United States; National Oceanic and Atmospheric Administration, Boulder, Colorado 80305, United States;* orcid.org/0000-0002-8399-5730; Email: Elizabeth.asher@noaa.gov

Authors

Alan J. Hills − *Atmospheric Chemistry Observations & Modeling Laboratory, National Center for Atmospheric Research, Boulder, Colorado 80301, United States*

Rebecca S. Hornbrook − *Atmospheric Chemistry Observations & Modeling Laboratory, National Center for Atmospheric Research, Boulder, Colorado 80301, United States*

Stephen Shertz − *Atmospheric Chemistry Observations & Modeling Laboratory, National Center for Atmospheric Research, Boulder, Colorado 80301, United States*

Stephen Gabbard − *Atmospheric Chemistry Observations & Modeling Laboratory, National Center for Atmospheric Research, Boulder, Colorado 80301, United States*

Britton B. Stephens − *Earth Observing Laboratory, National Center for Atmospheric Research, Boulder, Colorado 80301, United States*

Detlev Helmig − *Institute of Arctic and Alpine Research, University of Colorado, Boulder, Colorado 80309, United States*

Eric C. Apel − *Atmospheric Chemistry Observations & Modeling Laboratory, National Center for Atmospheric Research, Boulder, Colorado 80301, United States*

Complete contact information is available at: https://pubs.acs.org/10.1021/acs.est.0c07213

Notes

The authors declare no competing financial interest.
Data will be archived and made publicly available through NCAR's DASH database (https://dashrepo.ucar.edu/).

■ ACKNOWLEDGMENTS

The authors thank their 2018 summer engineering intern Alex Tilmes for his role as a WASPP remote pilot during anemometer intercomparison testing and for his role in design assistance; Laura Tudor for her help in calibrating sensors in the NCAR Earth Observing Laboratory; and Rudy Montoya for his construction of the custom electronic boards. This work was made possible by the Advanced Study Program at the National Center for Atmospheric Research. This material is based upon work supported by the National Center for Atmospheric Research, which is a major facility sponsored by the National Science Foundation under Cooperative Agreement no. 1852977.

■ REFERENCES

(1) World Health Organization. *World Health Statistics*; WHO: Geneva, Switzerland, 2018.
(2) EPA.gov. *Initial List of Hazardous Air Pollutants with Modifications. Environmental Topics: Air Topics*, https://www.epa.gov/haps/initial-list-hazardous-air-pollutants-modifications.
(3) Flocke, F.; Pfister, G.; Crawford, J. H.; Pickering, K. E.; Pierce, G.; Bon, D.; Reddy, P. Air Quality in the Northern Colorado Front Range Metro Area: The Front Range Air Pollution and Photochemistry Éxperiment (FRAPPÉ). *J. Geophys. Res.: Atmos.* **2020**, *125*, No. e2019JD031197.
(4) Stull, R. B., Ed. *An Introduction to Boundary Layer Meteorology*; Springer Netherlands: Dordrecht, 1988.
(5) Cooper, O. R.; Langford, A. O.; Parrish, D. D.; Fahey, D. W. Challenges of a Lowered U.S. Ozone Standard. *Science* **2015**, *348*, 1096−1097.
(6) Mathur, R.; Hogrefe, C.; Hakami, A.; Zhao, S.; Szykman, J.; Hagler, G. A Call for an Aloft Air Quality Monitoring Network: Need, Feasibility, and Potential Value. *Environ. Sci. Technol.* **2018**, *52*, 10903−10908.
(7) Apel, E. C.; Emmons, L. K.; Karl, T.; Flocke, F.; Hills, A. J.; Madronich, S.; Lee-Taylor, J.; Fried, A.; Weibring, P.; Walega, J.; Richter, D.; Tie, X.; Mauldin, L.; Campos, T.; Weinheimer, A.; Knapp, D.; Sive, B.; Kleinman, L.; Springston, S.; Zaveri, R.; Ortega, J.; Voss, P.; Blake, D.; Baker, A.; Warneke, C.; Welsh-Bon, D.; de Gouw, J.; Zheng, J.; Zhang, R.; Rudolph, J.; Junkermann, W.; Riemer, D. D. Chemical Evolution of Volatile Organic Compounds in the Outflow of the Mexico City Metropolitan Area. *Atmos. Chem. Phys.* **2010**, *10*, 2353−2375.
(8) Zhang, Y.; Dubey, M. K.; Olsen, S. C.; Zheng, J.; Zhang, R. Comparisons of WRF/Chem Simulations in Mexico City with Ground-Based RAMA Measurements during the 2006-MILAGRO. *Atmos. Chem. Phys.* **2009**, *9*, 3777−3798.
(9) Glaser, K. Vertical Profiles of O 3, NO 2, NO x, VOC, and Meteorological Parameters during the Berlin Ozone Experiment (BERLIOZ) Campaign. *J. Geophys. Res.* **2003**, *108*, No. 8253.
(10) Velasco, E.; Márquez, C.; Bueno, E.; Bernabé, R. M.; Sánchez, A.; Fentanes, O.; Wöhrnschimmel, H.; Cárdenas, B.; Kamilla, A.; Wakamatsu, S.; Molina, L. T. Vertical Distribution of Ozone and VOCs in the Low Boundary Layer of Mexico City. *Atmos. Chem. Phys.* **2008**, *8*, 3061−3079.
(11) Wofsy, S. C. HIAPER Pole-to-Pole Observations (HIPPO): Fine-Grained, Global-Scale Measurements of Climatically Important Atmospheric Gases and Aerosols. *Philos. Trans. R. Soc., A* **2011**, *369*, 2073−2086.
(12) Pétron, G.; Frost, G.; Miller, B. R.; Hirsch, A. I.; Montzka, S. A.; Karion, A.; Trainer, M.; Sweeney, C.; Andrews, A. E.; Miller, L.; Kofler, J.; Bar-Ilan, A.; Dlugokencky, E. J.; Patrick, L.; Moore, C. T.; Ryerson, T. B.; Siso, C.; Kolodzey, W.; Lang, P. M.; Conway, T.; Novelli, P.; Masarie, K.; Hall, B.; Guenther, D.; Kitzis, D.; Miller, J.; Welsh, D.; Wolfe, D.; Neff, W.; Tans, P. Hydrocarbon Emissions Characterization in the Colorado Front Range: A Pilot Study: COLORADO FRONT RANGE EMISSIONS STUDY. *J. Geophys. Res.: Atmos.* **2012**, *117*, No. D04304.
(13) Pétron, G.; Karion, A.; Sweeney, C.; Miller, B. R.; Montzka, S. A.; Frost, G. J.; Trainer, M.; Tans, P.; Andrews, A.; Kofler, J.; Helmig, D.; Guenther, D.; Dlugokencky, E.; Lang, P.; Newberger, T.; Wolter, S.; Hall, B.; Novelli, P.; Brewer, A.; Conley, S.; Hardesty, M.; Banta, R.; White, A.; Noone, D.; Wolfe, D.; Schnell, R. A New Look at Methane and Nonmethane Hydrocarbon Emissions from Oil and Natural Gas Operations in the Colorado Denver-Julesburg Basin: Hydrocarbon Emissions in Oil & Gas Basin. *J. Geophys. Res.: Atmos.* **2014**, *119*, 6836−6852.
(14) Asher, E.; Hornbrook, R. S.; Stephens, B. B.; Kinnison, D.; Morgan, E. J.; Keeling, R. F.; Atlas, E. L.; Schauffler, S. M.; Tilmes, S.; Kort, E. A.; Hoecker-Martínez, M. S.; Long, M. C.; Lamarque, J.-F.; Saiz-Lopez, A.; McKain, K.; Sweeney, C.; Hills, A. J.; Apel, E. C. Novel Approaches to Improve Estimates of Short-Lived Halocarbon Emissions during Summer from the Southern Ocean Using Airborne Observations. *Atmos. Chem. Phys.* **2019**, *19*, 14071−14090.
(15) Greenberg, J. Tethered Balloon Measurements of Biogenic VOCs in the Atmospheric Boundary Layer. *Atmos. Environ.* **1999**, *33*, 855−867.
(16) Wöhrnschimmel, H.; Márquez, C.; Mugica, V.; Stahel, W. A.; Staehelin, J.; Cárdenas, B.; Blanco, S. Vertical Profiles and Receptor Modeling of Volatile Organic Compounds over Southeastern Mexico City. *Atmos. Environ.* **2006**, *40*, 5125−5136.
(17) Dieu Hien, V. T.; Lin, C.; Thanh, V. C.; Kim Oanh, N. T.; Thanh, B. X.; Weng, C.-E.; Yuan, C.-S.; Rene, E. R. An Overview of the Development of Vertical Sampling Technologies for Ambient Volatile Organic Compounds (VOCs). *J. Environ. Manage.* **2019**, *247*, 401−412.
(18) Vo, T.-D.-H.; Lin, C.; Weng, C.-E.; Yuan, C.-S.; Lee, C.-W.; Hung, C.-H.; Bui, X.-T.; Lo, K.-C.; Lin, J.-X. Vertical Stratification of Volatile Organic Compounds and Their Photochemical Product Formation Potential in an Industrial Urban Area. *J. Environ. Manage.* **2018**, *217*, 327−336.
(19) Karion, A.; Sweeney, C.; Tans, P.; Newberger, T. AirCore: An Innovative Atmospheric Sampling System. *J. Atmos. Oceanic Technol.* **2010**, *27*, 1839−1853.
(20) Andersen, T.; Scheeren, B.; Peters, W.; Chen, H. A UAV-Based Active AirCore System for Measurements of Greenhouse Gases. *Atmos. Meas. Tech.* **2018**, *11*, 2683−2699.
(21) Chang, C.-C.; Wang, J.-L.; Chang, C.-Y.; Liang, M.-C.; Lin, M.-R. Development of a Multicopter-Carried Whole Air Sampling Apparatus and Its Applications in Environmental Studies. *Chemosphere* **2016**, *144*, 484−492.
(22) McKinney, K. A.; Wang, D.; Ye, J.; de Fouchier, J.-B.; Guimarães, P. C.; Batista, C. E.; Souza, R. A. F.; Alves, E. G.; Gu, D.; Guenther, A. B.; Martin, S. T. A Sampler for Atmospheric Volatile Organic Compounds by Copter Unmanned Aerial Vehicles. *Atmos. Meas. Tech.* **2019**, *12*, 3123−3135.
(23) Ore, J.-P.; Elbaum, S.; Burgin, A.; Detweiler, C. Autonomous Aerial Water Sampling: Autonomous Aerial Water Sampling. *J. Field Rob.* **2015**, *32*, 1095−1113.
(24) Sweeney, C. AirCore: The Answer to Making High-Precision Trace Gas Measurements on Remotely Operated Vehicles, International Society for Atmospheric Research using Remotely Piloted Aircraft, Boulder, CO,2018.

(25) Lampert, A.; Pätzold, F.; Asmussen, M. O.; Lobitz, L.; Krüger, T.; Rausch, T.; Sachs, T.; Wille, C.; Sotomayor Zakharov, D.; Gaus, D.; Bansmer, S.; Damm, E. Studying Boundary Layer Methane Isotopy and Vertical Mixing Processes at a Rewetted Peatland Site Using an Unmanned Aircraft System. *Atmos. Meas. Tech.* **2020**, *13*, 1937−1952.
(26) Greene, B.; Segales, A.; Bell, T.; Pillar-Little, E.; Chilson, P. Environmental and Sensor Integration Influences on Temperature Measurements by Rotary-Wing Unmanned Aircraft Systems. *Sensors* **2019**, *19*, No. 1470.
(27) Apel, E. C.; Hornbrook, R. S.; Hills, A. J.; Blake, N. J.; Barth, M. C.; Weinheimer, A.; Cantrell, C.; Rutledge, S. A.; Basarab, B.; Crawford, J.; Diskin, G.; Homeyer, C. R.; Campos, T.; Flocke, F.; Fried, A.; Blake, D. R.; Brune, W.; Pollack, I.; Peischl, J.; Ryerson, T.; Wennberg, P. O.; Crounse, J. D.; Wisthaler, A.; Mikoviny, T.; Huey, G.; Heikes, B.; O'Sullivan, D.; Riemer, D. D. Upper Tropospheric Ozone Production from Lightning NO x -Impacted Convection: Smoke Ingestion Case Study from the DC3 Campaign. *J. Geophys. Res.: Atmos.* **2015**, *120*, 2505−2523.
(28) Yoon, S.; Lee, H. C.; Pulliam, T. H. In *Computational Analysis of Multi-Rotor Flows*, 54th AIAA Aerospace Sciences Meeting, American Institute of Aeronautics and Astronautics: San Diego, California, 2016.
(29) Kolmogorov, A. N. The Local Structure of Turbulence in Incompressible Viscous Fluid for Very Large Reynolds Numbers. *Proc. R. Soc. London, Ser. A* **1941**, *434*, 9−13.
(30) Hubbard, K. G.; Lin, X.; Sun, B. Air Temperature Comparison between the MMTS and the USCRN Temperature Systems. *J. Atmos. Oceanic Technol.* **2004**, 1590−1597.
(31) Heidt, L. E. Whole Air Collection and Analysis. *Atmos. Technol.* **1978**, 3−7.
(32) Heidt, L. E.; Vedder, J. F.; Pollock, W. H.; Lueb, R. A.; Henry, B. E. Trace Gases in the Antarctic Atmosphere. *J. Geophys. Res.* **1989**, *94*, 11599.
(33) Schauffler, S. M.; Atlas, E. L.; Blake, D. R.; Flocke, F.; Lueb, R. A.; Lee-Taylor, J. M.; Stroud, V.; Travnicek, W. Distributions of Brominated Organic Compounds in the Troposphere and Lower Stratosphere. *J. Geophys. Res.: Atmos.* **1999**, *104*, 21513−21535.
(34) Apel, E.; Hornbrook, R.; Hills, A. *Trace Organic Gas Analyzer (TOGA) Data*, version 1.0, 2020, 16 data files, 1323 KiB; UCAR/NCAR, 2018. https://doi.org/doi:10.26023/F2JA-5WE7-ZH01.
(35) O'Dell, K.; Hornbrook, R. S.; Permar, W.; Levin, E. J. T.; Garofalo, L. A.; Apel, E. C.; Blake, N. J.; Jarnot, A.; Pothier, M. A.; Farmer, D. K.; Hu, L.; Campos, T.; Ford, B.; Pierce, J. R.; Fischer, E. V. Hazardous Air Pollutants in Fresh and Aged Western US Wildfire Smoke and Implications for Long-Term Exposure. *Environ. Sci. Technol.* **2020**, *54*, 11838−11847.
(36) Donnell, G. W.; Feight, J. A.; Lannan, N.; Jacob, J. D. In *Wind Characterization Using Onboard IMU of SUAS*, 2018 Atmospheric Flight Mechanics Conference, American Institute of Aeronautics and Astronautics: Atlanta, Georgia, 2018.
(37) Palomaki, R. T.; Rose, N. T.; van den Bossche, M.; Sherman, T. J.; De Wekker, S. F. J. Wind Estimation in the Lower Atmosphere Using Multirotor Aircraft. *J. Atmos. Oceanic Technol.* **2017**, *34*, 1183−1191.
(38) Rautenberg, A.; Graf, M.; Wildmann, N.; Platis, A.; Bange, J. Reviewing Wind Measurement Approaches for Fixed-Wing Unmanned Aircraft. *Atmosphere* **2018**, *9*, No. 422.
(39) Helmig, D. Air Quality Impacts from Oil and Natural Gas Development in Colorado. *Elementa: Sci. Anthropocene* **2020**, *8*, No. 4.
(40) Tanner, D.; Helmig, D.; Hueber, J.; Goldan, P. Gas Chromatography System for the Automated, Unattended, and Cryogen-Free Monitoring of C2 to C6 Non-Methane Hydrocarbons in the Remote Troposphere. *J. Chromatogr. A* **2006**, *1111*, 76−88.
(41) Halliday, H. S.; Thompson, A. M.; Wisthaler, A.; Blake, D. R.; Hornbrook, R. S.; Mikoviny, T.; Müller, M.; Eichler, P.; Apel, E. C.; Hills, A. J. Atmospheric Benzene Observations from Oil and Gas Production in the Denver-Julesburg Basin in July and August 2014: BENZENE OBSERVATIONS FROM OIL AND GAS. *J. Geophys. Res.: Atmos.* **2016**, *121*, 11055−11074.
(42) LeHau, H. H. Wind Profile, Surface Stress and Geostrophic Drag Coefficients in the Atmospheric Surface Layer. *Adv. Geophys.* **1959**, *6*, 241−257.
(43) Swarthout, R. F.; Russo, R. S.; Zhou, Y.; Hart, A. H.; Sive, B. C. Volatile Organic Compound Distributions during the NACHTT Campaign at the Boulder Atmospheric Observatory: Influence of Urban and Natural Gas Sources: VOLATILE ORGANIC COMPOUNDS DURING NACHTT. *J. Geophys. Res.: Atmos.* **2013**, *118*, 10614−10637.
(44) Gilman, J. B.; Lerner, B. M.; Kuster, W. C.; de Gouw, J. A. Source Signature of Volatile Organic Compounds from Oil and Natural Gas Operations in Northeastern Colorado. *Environ. Sci. Technol.* **2013**, *47*, 1297−1305.
(45) McDonald, B. C.; de Gouw, J. A.; Gilman, J. B.; Jathar, S. H.; Akherati, A.; Cappa, C. D.; Jimenez, J. L.; Lee-Taylor, J.; Hayes, P. L.; McKeen, S. A.; Cui, Y. Y.; Kim, S.-W.; Gentner, D. R.; Isaacman-VanWertz, G.; Goldstein, A. H.; Harley, R. A.; Frost, G. J.; Roberts, J. M.; Ryerson, T. B.; Trainer, M. Volatile Chemical Products Emerging as Largest Petrochemical Source of Urban Organic Emissions. *Science* **2018**, *359*, 760−764.
(46) Baker, A. K.; Beyersdorf, A. J.; Doezema, L. A.; Katzenstein, A.; Meinardi, S.; Simpson, I. J.; Blake, D. R.; Sherwood Rowland, F. Measurements of Nonmethane Hydrocarbons in 28 United States Cities. *Atmos. Environ.* **2008**, *42*, 170−182.
(47) Kumar, R.; Peuch, V.-H.; Crawford, J. H.; Brasseur, G. Five Steps to Improve Air-Quality Forecasts. *Nature* **2018**, *561*, 27−29.

https://doi.org/10.1021/acs.est.0c07213
Environ. Sci. Technol. 2021, 55, 5657−5667